DFT Studies of Solvent Effect on the Strongly Coupled Vibrations of 4-Azidoacetanilide

Sathya M. Perera and Lichang Wang[*]

School of Chemical and Biomolecular Sciences

Southern Illinois University Carbondale, Carbondale, IL 62901, USA

Abstract

DFT calculations were performed to study the solvent effect on the vibrations of 4-azidoacetanilde in the range including the azido asymmetric stretch, i.e. 2000-2300 cm^{-1}, using N, N-dimethylacetamide (NNDMA) and tetrahydrofuran (THF) as solvents. B3LYP functional was employed in the DFT calculations with 7 basis sets, 6-31G(d,p), 6-31+G(d,p), 6-31++G(d,p), 6-311G(d,p), 6-311+G(d,p), 6-311++G(d,p), and 6-311++G(df,pd). The results show that there are 7 combination bands coupling with the azide asymmetric stretch mode. As a result, the absorption profile of 4-azidoacetanilde is very solvent dependent. Specifically, stronger couplings of vibrations of 4-azidoacetanilde are predicted in NNDMA and the intensity of the azide asymmetric stretch is substantially reduced. Interestingly, the frequency of the azide asymmetric stretch of 4-azidoacetanilde in NNDMA is essentially the same as that of 4-azidotoulene. The intensity of the azide asymmetric stretch of 4-azidoacetanilde in THF is slightly increased with respect to that of 4-azidotoulene. Furthermore, the azide asymmetric stretch of 4-azidoacetanilde in THF remains nearly the same as in NNDMA but is blue shifted with respect to that of 4-azidotoulene. This indicates that a more complex and sensitive absorption profile will be expected when 4-azidoacetanilde is used as IR probe.

---

[*]Corresponding author: lwang@chem.siu.edu

1. Introduction

Organic azides have been widely studied for their role in participating in reactions[1] as well as as probes.[2-4] For instance, 4-azidotoluene and 4-azido-N-phenylmalemide were studied for the fermi resonance in the infrared spectra[5] as a part of the efforts to develop organic small molecule (OSM) based IR probes[5-11] to detect proteins[12-15] utilizing carbon-deuterium bond, nitrile, thiocyanate, azide, cyanamide, alkyne, or carbon-fluoride functional groups.[11,16-36] The facile synthesis of OSMs and the ability of fine tuning their properties of interest through functionalization have also made them promising materials in the development of solar cells,[37] luminescence[38] and fluorescence sensors.[39] Many OSM studies have therefore been carried out at the level of single molecules[40-74] as well as aggregates[37,75-98] to better understand the properties of these materials.

In the DFT studies on the IR spectra of 4-azidotoluene and 4-azido-N-phenylmalemide, we found that the vibrations of azido asymmetric stretch is closely coupled with other combination bands and is sensitive to the solvent. It will be interesting to further explore the effect of other functional groups on the IR spectrum of azido based molecules. Therefore, we carried out DFT calculations of 4-azidoacetanilde (as shown in Figure 1) in two solvents, N, N-dimethylacetamide (NNDMA) and tetrahydrofuran (THF). The objectives of the current work is twofold. The first is to further examine the influence of functional groups to the azido asymmetric stretch and the coupling strength of various modes. The second is to understand how solvent affect the IR spectrum and coupling among various vibrations. Similar to the previous studies of azido molecules, B3LYP functional was also employed in the current DFT calculations with 7 basis sets, 6-31G(d,p), 6-31+G(d,p), 6-31++G(d,p), 6-311G(d,p), 6-311+G(d,p), 6-311++G(d,p), and 6-

2

311++G(df,pd). Details of the computation are given in section 2. The results and discussion are provided in section 3 and the conclusions are drawn in section 4.
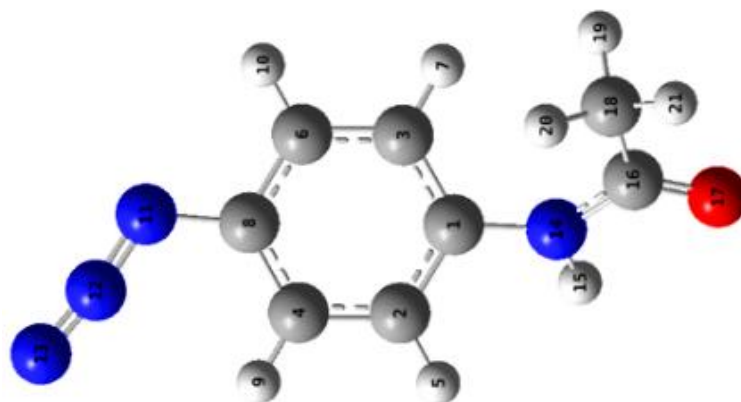

Figure 1. Chemical structure of 4-azidoacetanilde. The red, blue, gray, and white balls with numbers denote O, N, C, and H atoms, respectively.

2. Computational Details

All DFT calculations were carried out using Gaussian 16.[99] Geometry optimization and IR studies were performed for 4-azidoacetanilde in the same fashion as the previous studies of 4-azidotoluene and 4-azido-N-phenylmalemide.[5] In summary, B3LYP was used in all DFT calculations with seven basis sets, 6-31G(d,p), 6-31+G(d,p), 6-31++G(d,p), 6-311G(d,p), 6-311+G(d,p), 6-311++G(d,p), and 6-311++G(df,pd). Two solvents NNDM and THF were used to study the solvent effects. The polarizable continuum model using the integral equation formalism variant was used to include the solvent effect rather than the explicit solvent molecules. Standard convergence criteria were used in the DFT calculations, namely the self-consistent field, gradient, and energy convergence were set to be 10^{-8}, 10^{-4}, and 10^{-5} a.u., respectively. These convergence criteria have been also used in our previous work on other organic small molecules[100-104] as well

3

as DFT calculations of the other azido molecules.[5] We note that the harmonic frequency results showed that no imaginary frequencies for the optimized strcuture ensuring that it is at the minimum of the potential energy surface.

Anharmonic frequencies were obtained from the DFT calculations together with the cubic force constants of overtones and combination bands of 4-azidoacetanilide. To determine the Fermi Resonance (FR), we used both cubic coupling constants K_{ijk} and the third-order Fermi resonance parameter (TFR)[105,106] that was calculated by

$$\text{TFR} = \frac{|K_{ijk}|}{\Delta\omega}, \quad (1)$$

$$\Delta\omega = |\omega_i + \omega_j - \omega_k|, \quad (2)$$

where i, j, and k represents the fundamental mode. The combination band (or mode) of i and j is denoted as overtone when i=j. The combination modes (or bands) are considered resonant when TFR is of order ~1 or larger. To make sure all the possible couplings are included, we searched all the vibrational peaks of the molecule within ±130 cm^{-1} from the azido asymmetric stretch. The relative peak position ($\Delta\omega$') was calculated using

$$\Delta\omega' = \omega_{ij} - \omega_k, \quad (3)$$

where ω_{ij} and ω_k are the frequencies of combination band or overtone and the azido asymmetric stretch vibration, respectively.

3. Results and Discussion

In what follows, we will first present the geometric and electronic results of 4-azidoacetanilide in NNDMA and THF from the B3LYP/6-311+G(d,p) calculations. Then we will present the IR

4

spectra of the molecule in NNDMA and THF. Finally, we will discuss the solvent effect on the IR of 4-azidoacetanilide and compare the IR spectra with those of 4-azidotoluene. The structural parameters of 4-azidoacetanilide obtained from B3LYP/6-311+G(d,p), i.e. bond distances, bond angles, and dihedral angles, are summarized in Tables 1-3. The atoms are numbered according to the picture in Figure 1. In 4-azidoacetanilide, the azide group and benzene ring are in the same plane (D12 ≈ 180º). There are no significant changes in the bond distances and bond angles in two solvents. However, the dihedral angels of the D15, D16, D19, and D20 change slightly in different solvents.

Table 1. Bond distances (Å) of 4-azidoacetanilide in NNDMA and THF obtained from B3LYP/6-311+G(d,p) calculations.

Label	Definition	NNMDA	THF
R1	R(1,2)	1.399	1.399
R2	R(1,3)	1.399	1.399
R3	R(2,4)	1.390	1.390
R4	R(2,5)	1.084	1.084
R5	R(3,6)	1.389	1.389
R6	R(3,7)	1.082	1.082
R7	R(4,8)	1.399	1.399
R8	R(6,8)	1.397	1.397
R9	R(4,9)	1.084	1.084
R10	R(6,10)	1.083	1.083
R11	R(8,11)	1.421	1.420
R12	R(11,12)	1.231	1.231
R13	R(12,13)	1.133	1.133
R14	R(1,14)	1.421	1.420
R15	R(14,15)	1.013	1.013
R16	R(14,16)	1.370	1.372
R17	R(16,17)	1.231	1.229
R18	R(16,18)	1.511	1.512
R19	R(18,19)	1.093	1.093
R20	R(18,20)	1.090	1.090
R21	R(18,21)	1.089	1.089

5

Table 2. Bond angels of 4-azidoacetanilde in NNDMA and THF obtained from B3LYP/6-311+G(d,p) calculations

Label	Definition	NNDMA	THF
A1	A(1,2,3)	119.12	119.06
A2	A(1,2,4)	120.74	120.77
A3	A(1,2,5)	119.63	119.59
A4	A(1,3,6)	120.39	120.43
A5	A(1,3,7)	120.24	120.18
A6	A(2,4,8)	119.77	119.78
A7	A(3,6,8)	120.19	120.20
A8	A(2,4,9)	119.42	119.43
A9	A(3,6,10)	120.39	120.45
A10	A(4,8,11)	123.99	124.00
A11	A(6,8,11)	116.25	116.27
A12	A(8,11,12)	119.03	118.97
A13	A(11,12,13)	172.71	172.75
A14	A(1,3,14)	121.95	121.96
A15	A(1,14,15)	116.48	116.56
A16	A(1,14,16)	130.10	130.18
A17	A(14,16,17)	119.59	119.59
A18	A(14,16,18)	118.98	118.89
A19	A(16,18,19)	109.72	109.71
A20	A(16,18,20)	113.05	113.10
A21	A(16,18,21)	107.85	107.78

Table 3. Dihedral angels of 4-azidoacetanilde in NNDMA and THF obtained from B3LYP/6-311+G(d,p) calculations.

Label	Definition	NNDMA	THF
D1	D(4,2,1,3)	-0.56	-0.52
D2	D(5,2,1,3)	179.67	179.77
D3	D(6,3,1,2)	1.67	1.66
D4	D(7,3,1,2)	-177.31	-177.27
D5	D(8,4,2,1)	-0.72	-0.76
D6	D(8,6,3,1)	-1.50	-1.52
D7	D(9,4,2,1)	179.96	179.95

6

D8	D(10,6,3,1)	179.78	179.81
D9	D(2,4,8,11)	-179.51	-179.49
D10	D(3,6,8,11)	-179.42	-179.41
D11	D(4,8,11,12)	-0.29	-0.29
D12	D(6,8,11,12)	179.32	179.33
D13	D(8,11,12,13)	-179.84	-179.89
D14	D(6,3,1,14)	178.87	178.86
D15	D(3,1,14,15)	-135.10	-134.89
D16	D(1,14,16,17)	50.52	50.67
D17	D(1,14,16,18)	-179.24	-179.27
D18	D(14,16,18,19)	1.32	1.33
D19	D(14,16,18,20)	-91.86	-92.01
D20	D(14,16,18,21)	29.11	29.02

The DFT calculated frontier molecular orbitals, i.e. HOMO and LUMO, of 4-azidoacetanilide are illustrated in Figure 2. The HOMO and LUMO orbitals are the same in two solvents. The HOMO orbital is distributed in the region perpendicular to the bond axis avoiding all hydrogen atoms while the LUMO orbital is localized parallel to the bond axis and only covers the azide region and three carbon atoms close to the azide group. As the dihedral angles D15 and D16 slightly changed for both solvents due to the free bond rotation around single bonds. Hence, we expect that this will result in huge changes in the strength of the coupled vibrational modes consisting of the acetamide group.
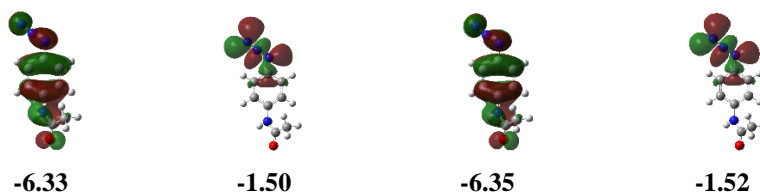

-6.33   -1.50   -6.35   -1.52

Figure 2. The spatial distributions of HOMO and LUMO molecular orbitals of 4-azidoacetanilide in NNDMA (left two) and THF (right two) obtained from B3LYP/6-311+G(d,p). The energies are in eV.

4-azidoacetanilide consists of 21 atoms. Thus, 57 (3N-6) fundamental vibrational modes can be observed in principle from the IR spectrum. The harmonic and anharmonic vibrational spectra of 4-azidoacetanilide with DFT/B3LYP/6-311+G(d,p) level in NNDMA are shown in Figure 3 with the vibrational modes with high intensities in the harmonic spectrum shown in Table 4. Data in Figure 3 and Table 4 shows that the azide asymmetric stretch (mode 49) has the highest intensity. Then, modes 48, 45, 40, 39, 38, and 37 have the next highest intensities. Hence, these vibrational modes are expected to most likely contribute to the FRs with azide asymmetric stretch.
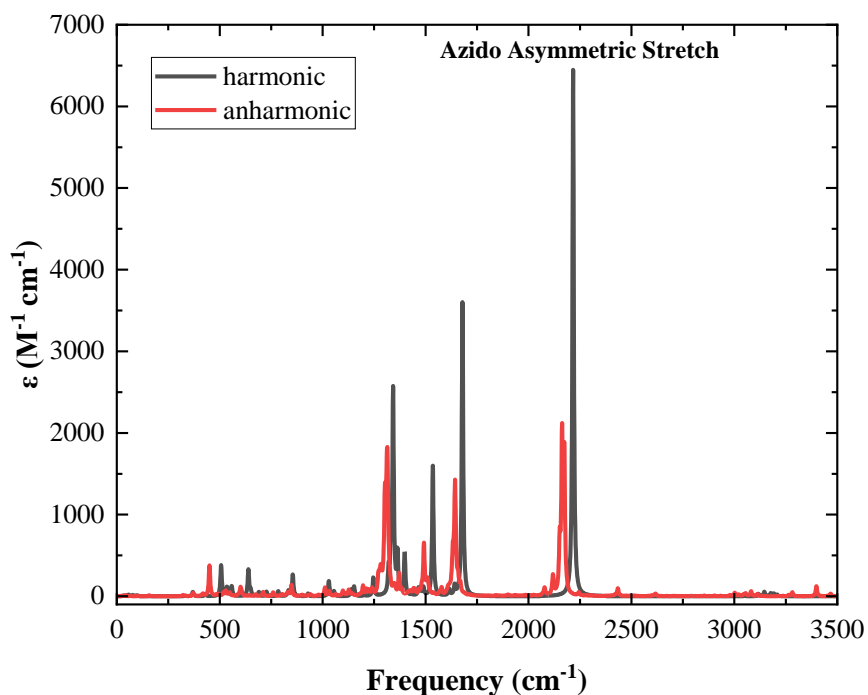
Figure 3. IR spectra of 4-azidoacetanilide in NNDMA from the B3LYP/6-311+G(d,p) calculations.

Table 4. Vibrational modes of 4-azidoacetanilide in NNDMA from B3LYP/6-311+G(d,p).

Mode	Vibration	$\upsilon_{(harmonic)}$ / cm^{-1}	$\upsilon_{(anharmonic)}$ / cm^{-1}	$I_{(harmonic)}$ / km mol^{-1}	$I_{(anharmonic)}$ / km mol^{-1}
49	N_3 asymmetric stretch	2216.9	2173.9	1868.1	475.4
48	C=O stretch, C-H in plane	1679.2	1643.2	1045.4	342.2
45	sp^2 C-H in-plane	1535.3	1492.0	463.9	169.8
40	sp^3 C-H oop	1398.4	1371.2	152.0	70.4
39	N_3 Sym stretch + C-N stretch + ring vibrations + C-H in-plane	1363.5	1315.6	143.0	61.3
38	C-N stretch + ring vibrations + C-H in-plane	1342.4	1305.8	716.4	2.5
37	sp^2 C-H in-plane	1332.5	1301.8	181.7	219.3

The anharmonic vibrational spectra of azide adsorption profile shown in Figure 3 shows a complex absorption profile, unlike those of 4-azidotoluene and 4-azidoacetanilide. Comb(20 45), Comb(22 41), and Comb(21 44) have the highest intensity. The high intensities for Comb(22 41) and Comb(16 48) modes which will be proven to be non-FRs later. The cubic force constants are shown for high-intensity peaks within the transparent window in Figure 4. Comb(24 39) has the highest cubic force constant around 50 cm^{-1}. But it is ~50 cm^{-1} away from the azide asymmetric stretch. Both Comb(22 39) and Over(33) have a cubic force constant of ~35 cm^{-1}, but they are also very far away from the fundamental vibration, ~80 and ~95 cm^{-1}, respectively. Then, Comb(24 38) has the cubic force constant > 10 cm^{-1}. However, it is also ~50 cm^{-1} away from the fundamental vibration. Both Comb(25 39) and Comb(24 40) are somewhat closer to the fundamental vibration with cubic force constant < 10 cm^{-1}. Hence, the intensity of these modes is not high from the vibrational coupling.
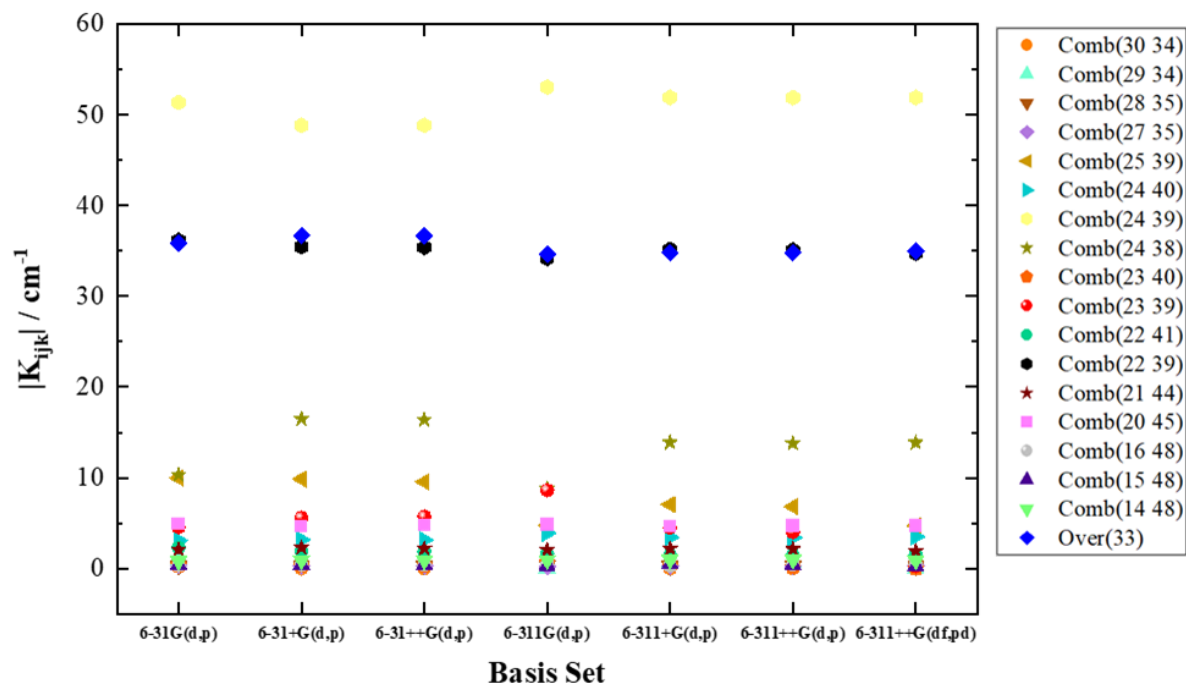
9

Figure 4. Cubic force constants of vibrational modes that can potentially couple with the azide asymmetric stretch of 4-azidoacetanilide in NNDMA obtained from B3LYP with 6-31G(d,p), 6-31+G(d,p), 6-31++G(d,p), 6-311G(d,p), 6-311+G(d,p), 6-311++G(d,p), 6-311++G(df,pd).

When $K_{ijk} < 10$ cm^{-1} and the vibrational mode is close to the fundamental vibration, there is still a chance to generate FRs. For example, Comb(20 45) is 10 cm^{-1} away from the azide asymmetric stretch except for the 6-31G(d,p) basis set, and has a cubic force constant of 5 cm^{-1}. Thus, Comb(20 45) has high intensity comparatively. When comparing the general trend of frequencies ($\Delta\omega'$) and resonance shift ($\Delta\omega$) of these FRs to the azide asymmetric stretch, they show the same pattern except for Comb(24 40) and Comb(20 45) due to the frequency is changing from $-\Delta\omega'$ to $+\Delta\omega'$ for double zeta to triple zeta basis sets. TFR values shown in Table 5 directly estimate what FRs are involved in complex azide adsorption profiles. However, lower $\Delta\omega$ values can give exceptionally high TFR values. For example, Comb(24 40) has a high TFR value of 17.5 due to a low $\Delta\omega$ of 0.2 cm^{-1}. To figure out FRs, the consistency of the TFR value is important. According to Table 3.17, only Comb(24 39) has TFR > 1. Hence, Comb(24 39) is strongly coupled to the azide asymmetric stretch.

10

Table 5. TFR values for the combination or overtone bands that may potentially couple with azide asymmetric stretch in 4-azidoacetanilide in NNDMA

| Mode	6-31G(d,p)	6-31+G(d,p)	6-31++G(d,p)	6-311G(d,p)	6-311+G(d,p)	6-311++G(d,p)	6-311++G(df,pd)
Over(33)	0.443	0.448	0.452	0.480	0.436	0.428	0.429
Comb(30 34)	0.056	0.000	0.000	0.028	0.000	0.000	0.020
Comb(29 34)	0.034	0.132	0.294	0.000	3.314	0.102	0.000
Comb(28 35)	0.006	0.019	0.022	0.008	0.015	0.050	0.175
Comb(27 35)	0.004	0.008	0.007	0.004	0.008	0.012	0.010
Comb(25 39)	0.354	0.474	0.403	0.104	0.783	0.423	0.344
Comb(24 40)	0.121	0.258	0.292	0.121	0.234	0.830	17.541
Comb(24 39)	0.863	1.022	1.040	2.539	1.267	1.224	1.475
Comb(24 38)	0.136	0.278	0.286	0.206	0.273	0.265	0.316
Comb(23 40)	0.006	0.009	0.008	0.021	0.843	0.018	0.000
Comb(23 39)	0.051	0.079	0.079	0.099	0.081	0.069	0.004
Comb(22 41)	0.080	0.064	0.059	0.077	0.053	0.068	0.072
Comb(22 39)	0.336	0.355	0.346	0.375	0.357	0.376	0.370
Comb(21 44)	0.100	0.047	0.045	0.135	0.045	0.051	0.078
Comb(20 45)	0.427	2.452	0.914	0.473	0.636	1.383	0.379
Comb(16 48)	0.004	0.011	0.013	0.007	0.022	0.078	0.005
Comb(15 48)	0.010	0.017	0.017	0.005	0.294	0.013	0.025
Comb(14 48)	0.016	0.055	0.047	0.007	0.012	0.011	0.351

Finally, Comb(20 45), Comb(25 39), Comb(22 39), and Over(33) were also considered being weakly coupled to the azide asymmetric stretch due to TFR > 0.3. Moreover, Comb(24 40) and Comb(24 38) can be also considered as FRs due to very weak coupling (TFR ≈ 0.3). Figure 5 illustrates individual normal modes that contribute to the FRs.
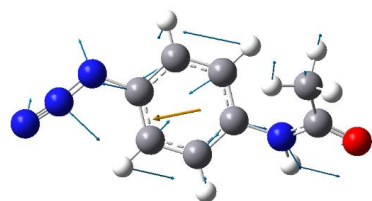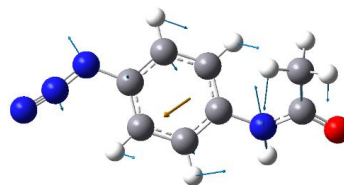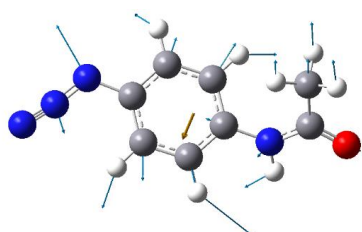
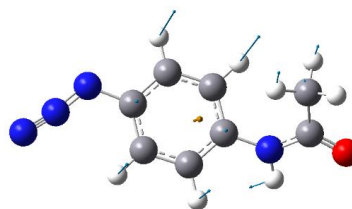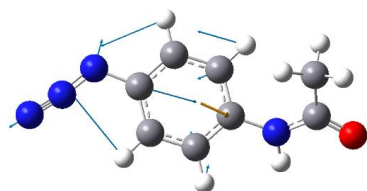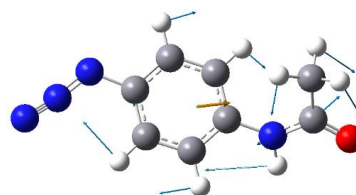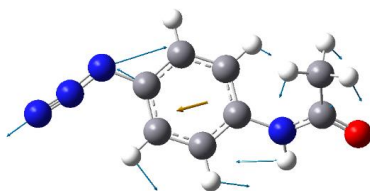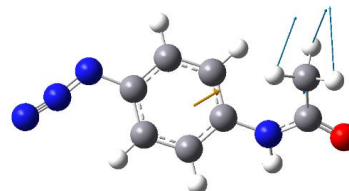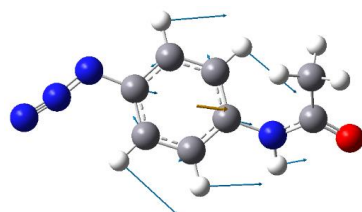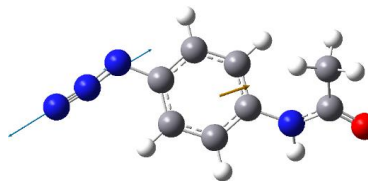**Figure 5**. Vibrational modes of combination or overtone bands that couple with azide asymmetric stretch in 4-azidoacetanilide.

We now discuss the solvent effect of 4-azidoacetanilide absorption profile that has shown to be complicated in NNDMA. Both harmonic and anharmonic spectra in THF are shown in Figure

6 and vibrational modes occurring within ±120 cm⁻¹ of the azide asymmetric stretch. Table 6 illustrates vibrational modes with high intensities in the harmonic spectrum. Anharmonic vibrational spectra of azide adsorption profile with seven different basis sets are shown in Figure 6. Like in the NNDMA solvent, 4-azidoacetanilide has a very complex absorption profile for the azide asymmetric stretch. As data in Figure 6 and Table 6 shown, the intensities of the vibrational modes change drastically, though the azido stretch remains nearly the same.
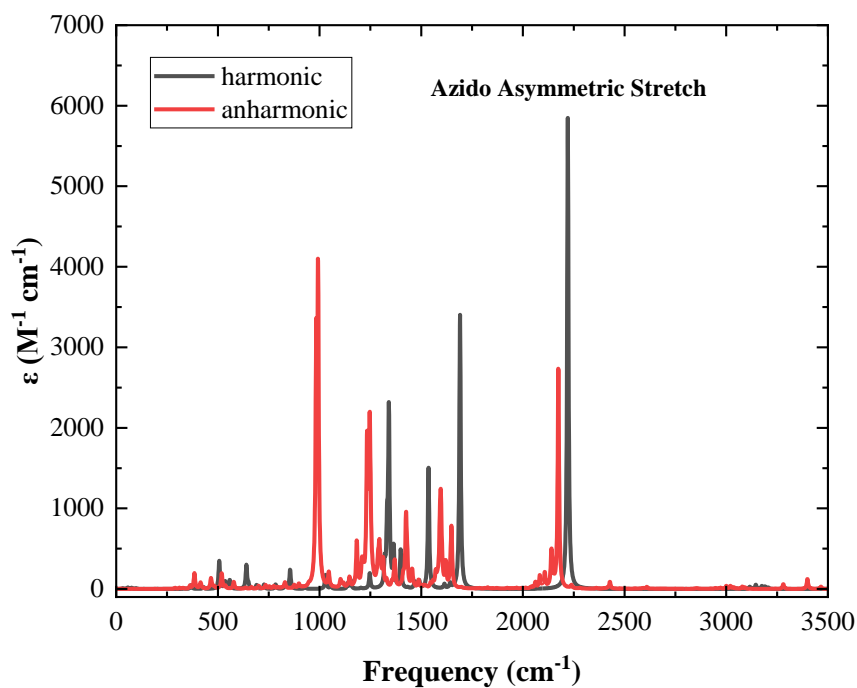

Figure 6. IR spectra of harmonic and anharmonic frequencies of 4-azidoacetanilide in THF obtained from B3LYP/6-311+G(d,p) calculations.

Table 6. Vibrational modes of 4-azidoacetanilide in THF using B3LYP/6-311+G(d,p)

Mode	Vibration	$\upsilon_{(harmonic)}$ / cm^{-1}	$\upsilon_{(anharmonic)}$ / cm^{-1}	$I_{(harmonic)}$ / km mol^{-1}	$I_{(anharmonic)}$ / km mol^{-1}
49	N_3 asymmetric stretch	2220.9	2174. 4	1693.0	795.2
48	C=O stretch, C-H in plane	1690.8	1684.5	986.4	135.7
45	sp^2 C-H in-plane	1535.9	1487.9	434.7	21.1
40	sp^3 C-H oop	1399.1	1355.1	136.0	17.5
39	N_3 Sym stretch + C-N stretch + ring vibrations + C-H in-plane	1364.5	1312.7	140.6	93.1
38	C-N stretch + ring vibrations + C-H in-plane	1340.9	1294.1	631.9	112.6
37	sp^2 C-H in-plane	1332.0	1233.6	193.5	478.1

Figure 7 presents the azide absorption profile of 4-azidoacetanilide in two solvents. The very striking feature of the two IR spectra is the frequency of the unchanged position of azido asymmetric stretch. Furthermore, much stronger coupling in NNDMA can be seen in Figure 7. These resulted in solvent dependent IR profiles. This can be illustrated clearly with the comparison to 4-azidotoulene in Figure 8. The extra peptide bond between the benzene ring and methyl group seems to complicate the azide absorption profile.
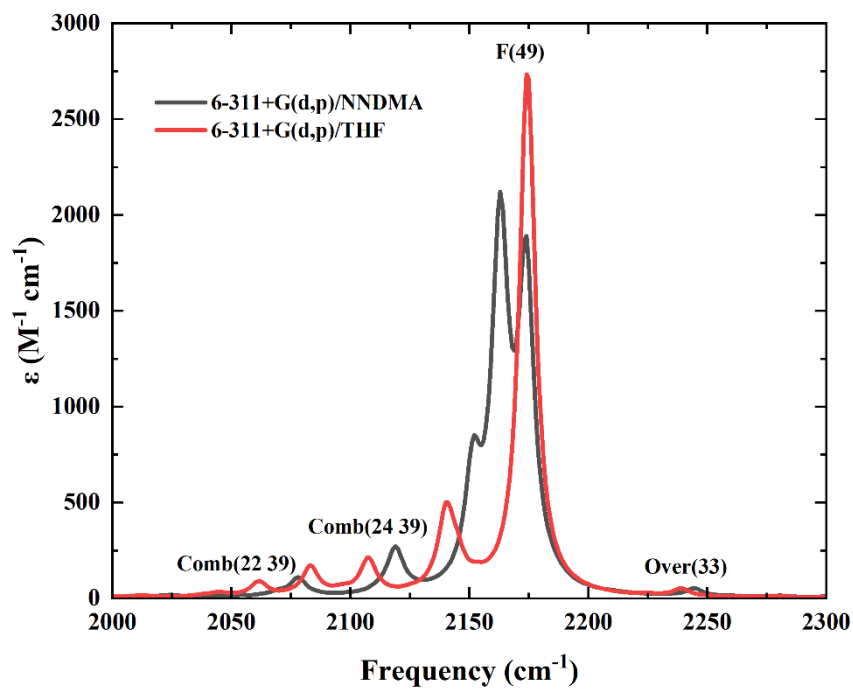
14

Figure 7. Vibrational spectra of 4-azidoacetanilide in NNDMA and THF obtained from B3LYP/6-311+G(d,p) calculations.
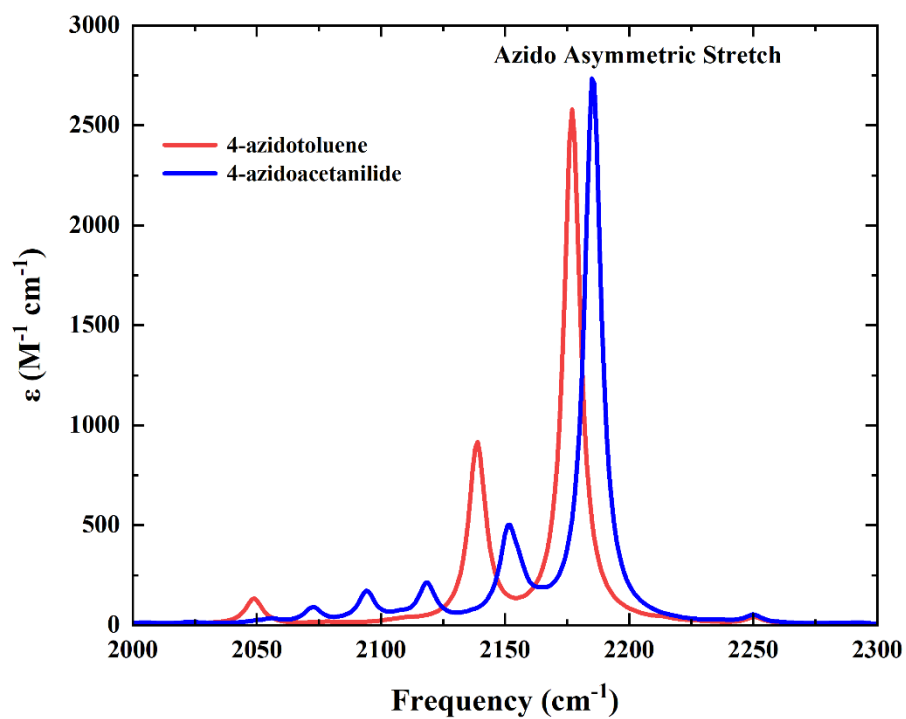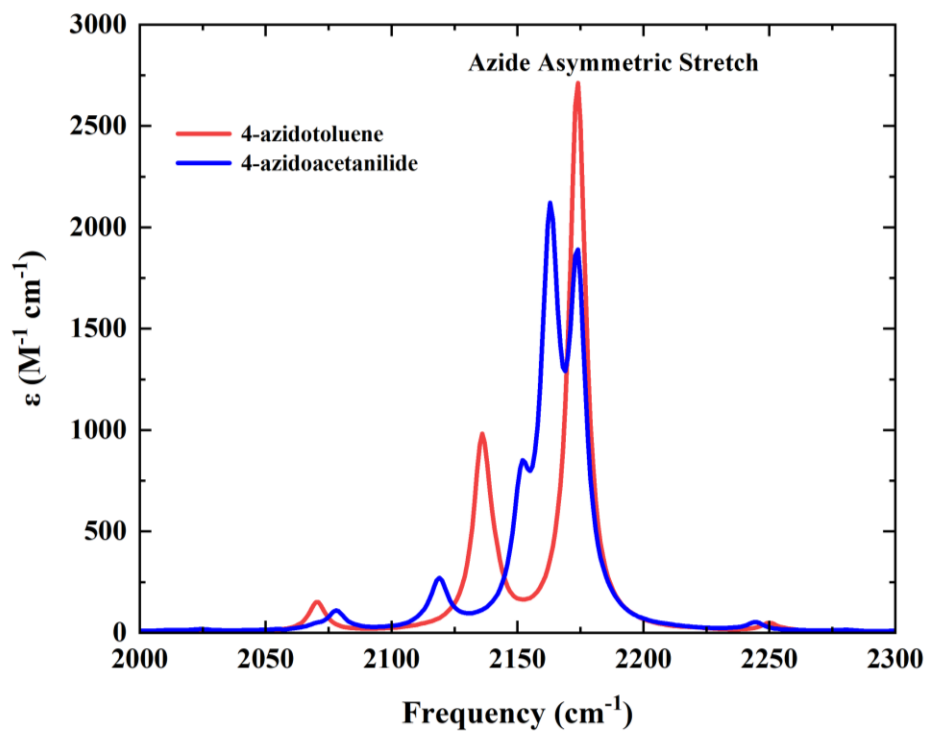
Figure 8. Vibrational spectra of 4-azidotoluene and 4-azidoacetanilide in NNDMA (top) and in THF (bottom) obtained from B3LYP/6-311+G(d,p). IR Data for 4-azidotoluene was taken from ref. 5.

16

We mention that results in THF using different basis set have similar impact as in NNDMA. The complication of absorption profile of 4-azidoacetanilde makes the difference in the results from different basis set larger. For example, 6-31+G(d,p) and 6-311G(d,p) basis sets have high intensity for Comb(20 45) and Comb(24 40), separately. Furthermore, Com(22 41) and Comb(21 44) have high intensity for triple zeta basis sets which will be proven to be non FRs due to low cubic force constant (~2 cm^{-1}) and longer $\Delta\omega'$ and $\Delta\omega$. Comb(15 48) has very high intensity (203 km/mol) in 6-311++G(df,pd) basis set while in other basis sets it is zero or less than 10 km/mol. Finally, we note that the single bonds will facilitate a lot of dynamic changes and performing dynamics studies[106-110] will be interesting to capture the dynamic aspects of the change and their impact in the IR spectra. Finally, synthesis of the azido molecules will active areas of research,[111-140] such as C-H[118-120,141] and C-C bond activations.[123,125,142]

4. Conclusions

To explore the potential of 4-azidoacetanilde as IR probe in the studies of proteins, we performed DFT calculations on the vibrations of 4-azidoacetanilde in the range of 2000-2300 cm^{-1} using N, N-dimethylacetamide (NNDMA) and tetrahydrofuran (THF) as solvents using B3LYP with seven basis sets, 6-31G(d,p), 6-31+G(d,p), 6-31++G(d,p), 6-311G(d,p), 6-311+G(d,p), 6-311++G(d,p), and 6-311++G(df,pd). The azido asymmetric stretch (mode 49) was found to differ only by about 0.5 cm^{-1} between NNDMA and less than 1 cm^{-1} in THF. However, the absorption profile differ greatly. The results show that there are 7 combination bands coupling with the azide asymmetric stretch mode. In comparison, there are 4 combination bands coupling with the azide asymmetric stretch mode of 4-azidotoulene.

The absorption profile of 4-azidoacetanilde is very solvent dependent. Specifically, stronger couplings of vibrations of 4-azidoacetanilde are predicted in NNDMA and the intensity of the

17

azide asymmetric stretch is substantially reduced. Interestingly, the frequency of the azide asymmetric stretch of 4-azidoacetanilde in NNDMA is essentially the same as that of 4-azidotoulene. The intensity of the azide asymmetric stretch of 4-azidoacetanilde in THF is slightly increased with respect to that of 4-azidotoulene. Furthermore, the azide asymmetric stretch of 4-azidoacetanilde in THF remains nearly the same but is blue shifted with respect to that of 4-azidotoulene. This indicates that a more complex and sensitive absorption profile will be expected when 4-azidoacetanilde is used as IR probe.

Finally, we point out that the strong couplings of various vibrational modes and the number of vibrations involved in 4-azidoacetanilde made the DFT results are very dependent on basis set. The magnitudes and the order of the cubic force constants among the vibrational modes vary greatly. Although these variations make the predictions challenging, they offer great opportunities to investigate the accuracy of basis sets in DFT calculations.

References

(1)   Agard, N. J.; Baskin, J. M.; Prescher, J. A.; Lo, A.; Bertozzi, C. R. *ACS Chem. Biol.* **2006**, *1*, 644.
(2)   Liu, F.; Chen, H.-M.; Armstrong, Z.; Withers, S. G. *ACS Cent. Sci.* **2022**, *8*, 656.
(3)   Bussink, A. P.; Swieten, P. F. v.; Ghauharali, K.; Scheij, S.; Eijk, M. v.; Wennekes, T.; Marel, G. A. v. d.; Boot, R. G.; Aerts, J. M. F. G.; Overkleeft, H. S. *J. Lipid Res.* **2007**, *48*, 1417.
(4)   Baskin, J. M.; Prescher, J. A.; Laughlin, S. T.; Agard, N. J.; Chang, P. V.; Miller, I. A.; Lo, A.; Codelli, J. A.; Bertozzi, C. R. *PNAS* **2007**, *104*, 16793.
(5)   Perera, S. M.; Aikawa, T.; Shaner, S. E.; Moran, S. D.; Wang, L. *ChemRxiv* **2022**, 10.26434/chemrxiv.
(6)   Baiz, C. R.; Błasiak, B.; Bredenbeck, J.; Cho, M.; Choi, J.-H.; Corcelli, S. A.; Dijkstra, A. G.; Feng, C.-J.; Garrett-Roe, S.; Ge, N.-H.; Hanson-Heine, M. W. D.; Hirst, J. D.; Jansen, T. L. C.; Kwac, K.; Kubarych, K. J.; Londergan, C. H.; Maekawa, H.; Reppert, M.; Saito, S.; Roy, S.; Skinner, J. L.; Stock, G.; Straub, J. E.; Thielges, M. C.; Tominaga, K.; Tokmakoff, A.; Torii, H.; Wang, L.; Webb, L. J.; Zanni, M. T. *Chem. Rev.* **2020**, *120*, 7152.
(7)   Brovarets, O. h. O.; Hovorun, D. M. *Chem. Phys. Impact* **2021**, *3*, 100033.
(8)   Mitra, S.; Khuu, T.; Choi, T. H.; Huchmala, R. M.; Jordan, K. D.; McCoy, A. B.; Johnson, M. A. *J. Phys. Chem. A* **2022**, *126*, 1640.
(9)   Ye, S.; Zaitseva, E.; Caltabiano, G.; Schertler, G. F. X.; Sakmar, T. P.; Deupi, X.; Vogel, R. *Nature* **2010**, *464*, 1386.
(10)   Perera, S. M.; Wang, L. *ChemRxiv* **2023**, 10.26434/chemrxiv.
(11)   Bazewicz, C. G.; Liskov, M. T.; Hines, K. J.; Brewer, S. H. *J. Phys. Chem. B* **2013**, *117*, 8987.
(12)   Thielges, M. C. *J. Chem. Phys.* **2021**, *155*, 040903.

(13)   Ma, J.; Pazos, I. M.; Zhang, W.; Culik, R. M.; Gai, F. *Annu. Rev. Phys. Chem.* **2015**, *66*, 357.

(14)   Kim, H.; Cho, M. *Chem. Rev.* **2013**, *113*, 5817.

(15)   Adhikary, R.; Zimmermann, J.; Romesberg, F. E. *Chem. Rev.* **2017**, *117*, 1927.

(16)   Cai, K.; Liu, J.; Liu, Y.; Chen, F.; Yan, G.; Lin, H. *Spectrochim Acta A Mol Biomol Spectrosc* **2020**, *227*, 117681.

(17)   Shi, L.; Liu, X.; Shi, L.; Stinson, H. T.; Rowlette, J.; Kahl, L. J.; Evans, C. R.; Zheng, C.; Dietrich, L. E. P.; Min, W. *Nat. Methods* **2020**, *17*, 844.

(18)   Lee, G.; Kossowska, D.; Lim, J.; Kim, S.; Han, H.; Kwak, K.; Cho, M. *J. Phys. Chem. B* **2018**, *122*, 4035.

(19)   Chalyavi, F.; Adeyiga, O.; Weiner, J. M.; Monzy, J. N.; Schmitz, A. J.; Nguyen, J. K.; Fenlon, E. E.; Brewer, S. H.; Odoh, S. O.; Tucker, M. J. *J. Chem. Phys.* **2020**, *152*, 074201.

(20)   Lam, Z.; Kong, K. V.; Olivo, M.; Leong, W. K. *Analyst* **2016**, *141*, 1569.

(21)   Bazewicz, C. G.; Lipkin, J. S.; Smith, E. E.; Liskov, M. T.; Brewer, S. H. *J. Phys. Chem. B* **2012**, *116*, 10824.

(22)   Wolfshorndl, M. P.; Baskin, R.; Dhawan, I.; Londergan, C. H. *J. Phys. Chem. B* **2012**, *116*, 1172.

(23)   Choi, J.-H.; Cho, M. *J. Chem. Phys.* **2011**, *134*, 154513.

(24)   Thielges, M. C.; Axup, J. Y.; Wong, D.; Lee, H. S.; Chung, J. K.; Schultz, P. G.; Fayer, M. D. *J. Phys. Chem. B* **2011**, *115*, 11294.

(25)   Gai, X. S.; Coutifaris, B. A.; Brewer, S. H.; Fenlon, E. E. *Phys. Chem. Chem. Phys.* **2011**, *13*, 5926.

(26)   Zheng, M. L.; Zheng, D. C.; Wang, J. *J. Phys. Chem. B* **2010**, *114*, 2327.

(27)   Fafarman, A. T.; Boxer, S. G. *J. Phys. Chem. B* **2010**, *114*, 13536.

(28)   Lee, H.; Choi, J.-H.; Cho, M. *Phys. Chem. Chem. Phys.* **2010**, *12*, 12658.

(29)   Waegele, M. M.; Tucker, M. J.; Gai, F. *Chem. Phys. Lett.* **2009**, *478*, 249.

(30)   Zimmermann, J.; Gundogdu, K.; Cremeens, M. E.; Bandaria, J. N.; Hwang, G. T.; Thielges, M. C.; Cheatum, C. M.; Romesberg, F. E. *J. Phys. Chem. B* **2009**, *113*, 7991.

(31)   Oh, K.-I.; Choi, J.-H.; Lee, J.-H.; Han, J.-B.; Lee, H.; Cho, M. *J. Chem. Phys.* **2008**, *128*, 154504.

(32)   Choi, J.-H.; Oh, K.-I.; Lee, H.; Lee, C.; Cho, M. *J. Chem. Phys.* **2008**, *128*, 134506.

(33)   Fafarman, A. T.; Webb, L. J.; Chuang, J. I.; Boxer, S. G. *J. Am. Chem. Soc.* **2006**, *128*, 13356.

(34)   Deiters, A.; Schultz, P. G. *Bioorg. Med. Chem. Lett.* **2005**, *15*, 1521.

(35)   Getahun, Z.; Huang, C. Y.; Wang, T.; De León, B.; DeGrado, W. F.; Gai, F. *J Am Chem Soc* **2003**, *125*, 405.

(36)   Chin, J. K.; Jimenez, R.; Romesberg, F. E. *J. Am. Chem. Soc.* **2001**, *123*, 2426.

(37)   Xu, F.; Gong, K.; Liu, D.; Wang, L.; Li, W.; Zhou, X. *Solar Energy* **2022**, *240*, 157.

(38)   Wang, T.; Liu, M.; Feng, W.; Cao, R.; Sun, Y.; Wang, L.; Liu, D.; Wang, Y.; Wang, T.; Hu, W. *Adv. Opt. Mater.* **2023**, *11*, 2202613.

(39)   McCarroll, M. E.; Shi, Y.; Harris, S.; Puli, S.; Kimaru, I.; Xu, R.; Wang, L.; Dyer, D. J. *J. Phys. Chem. B* **2006**, *110*, 22991.

(40)   Sumithra, M.; Sundaraganesan, N.; Rajesh, R.; Vetrivelan, V.; Ilangovan, V.; Javed, S.; Muthu, S. *Chem. Phys. Impact* **2023**, *6*, 100145.

(41)   Zhou, X.; Liu, D.; Wang, T.; Hu, X.; Guo, J.; Weerasinghe, K. C.; Wang, L.; Li, W. *J. Photochem. Photobiol. A: Chem.* **2014**, *274*, 57.

(42)   Wang, T.; Zhao, C.; Zhang, L.; Lu, T.; Sun, H.; Bridgmohan, C. N.; Weerasinghe, K. C.; Liu, D.; Hu, W.; Li, W.; Zhou, X.; Wang, L. *J. Phys. Chem. C* **2016**, *120*, 25263.

(43)   Wang, T.; Weerasinghe, K. C.; Sun, H.; Hu, X.; Lu, T.; Liu, D.; Hu, W.; Li, W.; Zhou, X.; Wang, L. *J. Phys. Chem. C* **2016**, *120*, 11338.

(44)   Sun, H.; Liu, D.; Wang, T.; Lu, T.; Li, W.; Ren, S.; Hu, W.; Wang, L.; Zhou, X. *ACS Appl. Mater. Interfaces* **2017**, *9*, 9880.

(45)   Wang, T.; Weerasinghe, K. C.; Ubaldo, P. C.; Liu, D.; Li, W.; Zhou, X.; Wang, L. *Chem. Phys. Lett.* **2015**, *618*, 142.

(46)   Wang, T.; Liu, M.; Gao, C.; Song, Y.; Wang, L.; Liu, D.; Wang, T.; Hu, W. *Dyes Pigm.* **2022**, *207*, 110734.

(47)   Liu, M.; Muleta, D. Y.; Yu, Z.; Wang, L.; Liu, D.; Wang, T.; Hu, W. *J. Mater. Chem. C* **2022**, *10*, 12249.

(48)   Wang, R.; Gong, K.; Liu, R.; Liu, D.; Li, W.; Wang, L.; Zhou, X. *J. Porphyrins Phthalocyanines* **2022**, *26*, 469.

(49)   Gong, K.; Yang, J.; Testoff, T. T.; Li, W.; Wang, T.; Liu, D.; Zhou, X.; Wang, L. *Chem. Phys.* **2021**, *549*, 111256.

(50)   Ge, F.; Xu, F.; Gong, K.; Liu, D.; Li, W.; Wang, L.; Zhou, X. *Dyes Pigm.* **2022**, *200*, 110127.

(51)   Song, J.; Muleta, D. Y.; Feng, W.; Song, Y.; Zhou, X.; Li, W.; Wang, L.; Liu, D.; Wang, T.; Hu, W. *Dyes Pigm.* **2021**, *193*, 109501.

(52)   Weerasinghe, K. C.; Wang, T.; Zhuang, J.; Sun, H.; Liu, D.; Li, W.; Hu, W.; Zhou, X.; Wang, L. *Chem. Phys. Impact* **2022**, *4*, 100062.

(53)   Feng, W.; Wang, T.; Testoff, T. T.; Bridgmohan, C. N.; Zhao, C.; Sun, H.; Hu, W.; Li, W.; Liu, D.; Wang, L.; Zhou, X. *Spectrochim. Acta. Part A* **2020**, *229*, 118016.

(54)   Yang, J.; Liu, D.; Lu, T.; Sun, H.; Li, W.; Testoff, T. T.; Zhou, X.; Wang, L. *Int. J. Quantum Chem.* **2020**, *120*, e26355.

(55)   Sun, H.; Li, P.; Liu, D.; Wang, T.; Li, W.; Hu, W.; Wang, L.; Zhou, X. *J. Photochem. Photobiol. A: Chem.* **2019**, *368*, 233.

(56)   Muleta, D. Y.; Song, J.; Feng, W.; Wu, R.; Zhou, X.; Li, W.; Wang, L.; Liu, D.; Wang, T.; Hu, W. *J. Mater. Chem. C* **2021**, *9*, 5093.

(57)   Lukasak, B.; Morihiro, K.; Deiters, A. *Sci. Rep.* **2019**, *9*, 1470.

(58)   Kumar, N. S.; Prasad, K. N. N.; Chandrasekhar, S.; Thipperudrappa, J. *Chem. Phys. Impact* **2023**, *6*, 100136.

(59)   Zheng, Y.; Chen, Y.; Cao, Y.; Huang, F.; Guo, Y.; Zhu, X. *ACS Mater. Lett.* **2022**, *4*, 882.

(60)   Zhao, M.; Wei, Q.; Zhang, J.; Li, W.; Wang, Z.; Du, S.; Xue, Q.; Xie, G.; Ge, Z. *Org. Electronics* **2022**, *100*, 106365.

(61)   Zeng, L.; Huang, L.; Han, J.; Han, G. *Acc. Chem. Res.* **2022**, *55*, 2604.

(62)   Yashwantrao, G.; Saha, S. *Dyes Pigm.* **2022**, *199*, 110093.

(63)   Xu, C.; Zhao, Z.; Yang, K.; Niu, L.; Ma, X.; Zhou, Z.; Zhang, X.; Zhang, F. *J. Mater. Chem. A* **2022**, *10*, 6291.

(64)   Wang, Y.; Wang, X.; Ma, W.; Lu, R.; Zhou, W.; Gao, H. *Chemosensors* **2022**, *10*, 399.

(65)   Walia, R.; Yang, J. *Photochem. Photobiol. Sci.* **2022**, *21*, 1689.

(66)   Sharif, O. F. A.; Nhari, L. M.; El-Shishtawy, R. M.; Zayeda, M. E. M.; Asiri, A. M. *RSC Adv.* **2022**, *12*, 19270.

(67)   Nagaraju, N.; Kushavah, D.; Kumar, S.; Ray, R.; Gambhir, D.; Ghosh, S.; Pal, S. K. *Phys. Chem. Chem. Phys.* **2022**, *24*, 3303.

(68)   Malik, M. Y. H.; Binyamin, M. A.; Hayat, S. *Polycyclic Aromat. Compd.* **2022**, *42*, 6267.

(69)   Loong, H.; Zhou, J.; Jiang, N.; Feng, Y.; Xie, G.; Liu, L.; Xie, Z. *J. Phys. Chem. B* **2022**, *126*, 2441.

(70)   Li, J.; Dong, Y.; Wei, R.; Jiang, G.; Yao, C.; Lv, M.; Wu, Y.; Gardner, S. H.; Zhang, F.; Lucero, M. Y.; Huang, J.; Chen, H.; Ge, G.; Chan, J.; Chen, J.; Sun, H.; Luo, X.; Qian, X.; Yang, Y. *J. Am. Chem. Soc.* **2022**, *144*, 14351.

(71)   Koteshwar, D.; Prasanthkumar, S.; Singh, S. P.; Chowdhury, T. H.; Bedja, I.; Islam, A.; Giribabu, L. *Mater. Chem. Front.* **2022**, *6*, 580.

(72)   Kong, D.; Cai, T.; Fan, H.; Hu, H.; Wang, X.; Cui, Y.; Wang, D.; Wang, Y.; Hu, H.; Wu, M.; Xue, Q.; Yan, Z.; Li, X.; Zhao, L.; Xing, W. *Angew. Chem., Int. Ed.* **2022**, *61*, e202114681.

(73)   Khan, Q. U.; Begum, N.; Khan, K.; Rauf, M.; Zhan, Y. *Org. Electron.* **2022**, *103*, 106453.

(74)   He, Q.; Dong, F.; Xing, L.; He, H.; Chen, X.; Wang, H.; Ji, S.; Huo, Y. *Tetrahedron* **2022**, *104*, 132565.

(75)   Xu, F.; Testoff, T. T.; Wang, L.; Zhou, X. *Molecules* **2020**, *25*, 4478.

(76)   Testoff, T. T.; Aikawa, T.; Tsung, E.; Lesko, E.; Wang, L. *Chem. Phys.* **2022**, *562*, 111641.

(77)   Xu, F.; Gong, K.; Fan, W.; Liu, D.; Li, W.; Wang, L.; Zhou, X. *ACS Appl. Energy Mater.* **2022**, *5*, 13780.

(78)   Liu, R.; Liu, D.; Meng, F.; Li, W.; Wang, L.; Zhou, X. *Dyes Pigm.* **2021**, *187*, 109135.

(79)   Zhao, J.; Zheng, X. *Front. Chem.* **2022**, *9*, 808957.

(80)   Wang, L.; Liu, Y.-L.; Li, Q.-J.; Chen, S.-H.; He, D.; Wang, M.-S. *J. Phys. Chem. A* **2022**, *126*, 870.

(81)   Waly, S. M.; Karlsson, J. K. G.; Waddell, P. G.; Benniston, A. C.; Harriman, A. *J. Phys. Chem. A* **2022**, *126*, 1530–1541.

(82)   Sun, S.; Conrad-Burton, F. S.; Liu, Y.; Ng, F.; Steigerwald, M.; Zhu, X.; Nuckolls, C. *J. Phys. Chem. A* **2022**, *126*, 7559.

(83)   Pradeep, V. V.; Chandrasekar, R. *Adv. Opt. Mater.* **2022**, *10*, 2201150.

(84)   Parida, S.; Patra, S. K.; Mishra, S. *ChemPhysChem* **2022**, *23*, e202200361.

(85)   Kuimov, A. D.; Becker, C. S.; Sonina, A. A.; Kazantsev, M. S. *New J. Chem.* **2022**, *46*, 21257.

(86)   Kousseff, C. J.; Halaksa, R.; Parr, Z. S.; Nielsen, C. B. *Chem. Rev.* **2022**, *122*, 4397.

(87)   Hai, T.; Feng, Z.; Sun, Y.; Wong, W.-Y.; Liang, Y.; Zhang, Q.; Lei, Y. *ACS Nano* **2022**, *16*, 3290.

(88)   Cheng, Q.; Hao, A.; Xing, P. *ACS Nano* **2022**, *16*, 6825.

(89)   Bernhardt, R.; Manrho, M.; Zablocki, J.; Rieland, L.; Lützen, A.; Schiek, M.; Meerholz, K.; Zhu, J.; Jansen, T. L. C.; Knoester, J.; Loosdrecht, P. H. M. v. *J. Am. Chem. Soc.* **2022**, *144*, 19372–19381.

(90)   Afraj, S. N.; Lin, C.-C.; Velusamy, A.; Cho, C.-H.; Liu, H.-Y.; Chen, J.; Lee, G.-H.; Fu, J.-C.; Ni, J.-S.; Tung, S.-H.; Yau, S.; Liu, C.-L.; Chen, M.-C.; Facchetti, A. *Adv. Funct. Mater.* **2022**, *32*, 2200880.

(91)   Zhou, Q.; Lei, Y.; Fu, H. *J. Mater. Chem. C* **2021**, *9*, 489.

(92)   Zhang, Y.-Y.; Qiu, F.-Y.; Shi, H.-T.; Yu, W. *Chem. Commun.* **2021**, *57*, 3010.

(93)   Zhang, Y.; Zhu, L.; Tian, J.; Zhu, L.; Ma, X.; He, X.; Huang, K.; Ren, F.; Xu, W. *Adv. Sci.* **2021**, *8*, 2100216.

(94)   Zhang, P.-F.; Zeng, J.-C.; Zhuang, F.-D.; Zhao, K.-X.; Sun, Z.-H.; Yao, Z.-F.; Lu, Y.; Wang, X.-Y.; Wang, J.-Y.; Pei, J. *Angew. Chem., Int. Ed.* **2021**, *60*, 23313.

(95)   Wu, R.; Wang, Y.; Zhu, Z.; Yu, C.; Li, H.; Li, B.; Dong, S. *ACS Appl. Mater. Interfaces* **2021**, *13*, 9482.

(96)   Wang, Y.; Qin, W. *Org. Electron.* **2021**, *92*, 106103.

(97)   Wang, J.; Xu, S.; Zhang, H.; Chen, L.; Guan, S.; Xu, W. *Cryst. Growth Des.* **2021**, *21*, 2699.

(98)   Song, J.; Muleta, D. Y.; Feng, W.; Song, Y.; Zhou, X.; Li, W.; Wang, L.; Liu, D.; Wang, T.; Hu, W. *Dye Pigm.* **2021**, *193*, 109501.

(99)   Frisch, M. J.; Trucks, G. W.; Schlegel, H. B.; Scuseria, G. E.; Robb, M. A.; Cheeseman, J. R.; Scalmani, G.; Barone, V.; Petersson, G. A.; Nakatsuji, H.; Li, X.; Caricato, M.; Marenich, A. V.; Bloino, J.; Janesko, B. G.; Gomperts, R.; Mennucci, B.; Hratchian, H. P.; Ortiz, J. V.; Izmaylov, A. F.; Sonnenberg, J. L.; Williams; Ding, F.; Lipparini, F.; Egidi, F.; Goings, J.; Peng, B.; Petrone, A.; Henderson, T.; Ranasinghe, D.; Zakrzewski, V. G.; Gao, J.; Rega, N.; Zheng, G.; Liang, W.; Hada, M.; Ehara, M.; Toyota, K.; Fukuda, R.; Hasegawa, J.; Ishida, M.; Nakajima, T.; Honda, Y.; Kitao, O.; Nakai, H.; Vreven, T.; Throssell, K.; Montgomery Jr., J. A.; Peralta, J. E.; Ogliaro, F.; Bearpark, M. J.; Heyd, J. J.; Brothers, E. N.; Kudin, K. N.; Staroverov, V. N.; Keith, T. A.; Kobayashi, R.; Normand, J.; Raghavachari, K.; Rendell, A. P.; Burant, J. C.; Iyengar, S. S.; Tomasi, J.; Cossi, M.; Millam, J. M.; Klene, M.; Adamo, C.; Cammi, R.; Ochterski, J. W.; Martin, R. L.; Morokuma, K.; Farkas, O.; Foresman, J. B.; Fox, D. J. Wallingford, CT, 2016.

(100)   Walkup, L. L.; Weerasinghe, K. C.; Tao, M.; Zhou, X.; Zhang, M.; Liu, D.; Wang, L. *J. Phys. Chem. C* **2010**, *114*, 19521.

(101)   Hudson, G. A.; Cheng, L.; Yu, J.; Yan, Y.; Dyer, D. J.; McCarroll, M. E.; Wang, L. *J. Phys. Chem. B* **2010**, *114*, 870.

(102)   Wang, T.; Weerasinghe, K. C.; Liu, D.; Li, W.; Yan, X.; Wang, X. Z. L. *J Mater. Chem. C* **2014**, *2*, 5466.

(103)   Lin, T.; Zhang, W.; Wang, L. *J. Phys. Chem. A* **2009**, *113* 7267.

(104)   Lin, T.; Zhang, W.; Wang, L. *J. Phys. Chem. A* **2008**, *112*, 13600.

(105)   Pandey, H. D.; Leitner, D. M. *J. Phys. Chem. A* **2018**, *122*, 6856.

(106) Fujisaki, H.; Yagi, K.; Hirao, K.; Straub, J. E. *Chem. Phys. Lett.* **2007**, *443*, 6.

(107) Wang, L.; Kalyanaraman, C.; McCoy, A. B. *J. Chem. Phys.* **1999**, *110*, 11221.

(108) Sotome, H.; Koga, M.; Sawada, T.; Miyasaka, H. *Phys. Chem. Chem. Phys.* **2022**, *24*, 14187.

(109) Rumble, C. A.; Vauthey, E. *J. Phys. Chem. B* **2021**, *125*, 10527.

(110) Qin, S.; Meng, L.; Li, Y. *ACS Omega* **2021**, *6*, 14467.

(111) Sun, K.; Zhang, M.; Wang, L. *Chem. Phys. Lett.* **2013**, *585*, 89.

(112) Lu, J.; Aydin, C.; Browning, N. D.; Wang, L.; Gates, B. C. *Catal. Lett.* **2012**, *142*, 1445.

(113) Wang, L.; Williams, J. I.; Lin, T.; Zhong, C. J. *Catal. Today* **2011**, *165*, 150.

(114) Xu, H.; Miao, B.; Zhang, M.; Chen, Y.; Wang, L. *Phys. Chem. Chem. Phys.* **2017**, *19*, 26210.

(115) Wu, Z.; Zhang, M.; Jiang, H.; Zhong, C.-J.; Chen, Y.; Wang, L. *Phys. Chem. Chem. Phys.* **2017**, *19*, 15444.

(116) Miao, B.; Wu, Z.-P.; Xu, H.; Zhang, M.; Chen, Y.; Wang, L. *Comput. Mater. Sci.* **2019**, *156*, 175.

(117) Miao, B.; Wu, Z.; Xu, H.; Zhang, M.; Chen, Y.; Wang, L. *Chem. Phys. Lett.* **2017**, *688*, 92.

(118) Wu, R.; Wang, L. *J. Phys. Chem. C* **2022**, *126*, 21650.

(119) Wu, R.; Wang, L. *Chem. Phys. Impact* **2021**, *3*, 100040.

(120) Wu, R.; Wang, L. *ChemPhysChem* **2022**, *23*, e202200132.

(121) Wu, R.; Wang, L. *Phys. Chem. Chem. Phys.* **2023**, *25*, 2190.

(122) Wu, C.; Wang, L.; Xiao, Z.; Li, G.; Wang, L. *Phys. Chem. Chem. Phys.* **2020**, *22*, 724.

(123) Wu, R.; Wiegand, K. R.; Ge, L.; Wang, L. *J. Phys. Chem. C* **2021**, *125*, 14275.

(124) Wang, L.; Ore, R. M.; Jayamaha, P. K.; Wu, Z.-P.; Zhong, C.-J. *Faraday Discuss.* **2023**, *242*, 429.

(125) Wu, R.; Wang, L. *J. Phys. Chem. C* **2020**, *124*, 26953.

(126) Wu, R.; Sun, K.; Chen, Y.; Zhang, M.; Wang, L. *Surf. Sci.* **2021**, *703*, 121742.

(127) Wu, R.; Wang, L. *Comput. Mater. Sci.* **2021**, *196*, 110514.

(128) Hajipour, A. R.; Mohammadsaleh, F. *Tetrahedron Lett.* **2014**, *55*, 6799.

(129) Pettipas, R. D.; Hoff, A.; Gelfand, B. S.; Welch, G. C. *ACS Appl. Mater. Interfaces* **2022**, *14*, 3103.

(130) Wang, Y.-H.; Wang, L.-T.; Yao, Z.-Z.; Yin, J.-J.; Huang, Z.-B.; Yuan, P.-Q.; Yuan, W.-K. *Chem. Eng. Sci.* **2021**, *232*, 116342.

(131) Watanabe, H.; Takemoto, M.; Adachi, K.; Okuda, Y.; Dakegata, A.; Fukuyama, T.; Ryu, I.; Wakamatsu, K.; Orita, A. *Chem. Lett.* **2020**, *49*, 409.

(132) Ruppel, M.; Gazetas, L.-P.; Lungerich, D.; Jux, N. *Eur. J. Org. Chem.* **2020**, 6352.

(133) Pigulski, B.; Ximenis, M.; Shoyama, K.; Wuerthner, F. *Org. Chem. Front.* **2020**, *7*, 2925.

(134) Markl, J. S.; Mueller, W. E. G.; Sereno, D.; Elkhooly, T. A.; Kokkinopoulou, M.; Garderes, J.; Depoix, F.; Wiens, M. *Biotechnol. Bioeng.* **2020**, *117*, 1789.

(135) Huang, Y.; Gong, Q.; Ge, J.; Tang, P.; Yu, F.; Xiao, L.; Wang, Z.; Sun, H.; Yu, J.; Li, D.-S.; Xiong, Q.; Zhang, Q. *ACS Nano* **2020**, *14*, 15962.

(136) Zhao, C.; Wang, T.; Li, D.; Lu, T.; Liu, D.; Meng, Q.; Zhang, Q.; Li, F.; Li, W.; Hu, W.; Wang, L.; Zhou, X. *Dye Pigm.* **2017**, *137*, 256.

(137) Li, J.; Ballmer, S. G.; Gillis, E. P.; Fujii, S.; Schmidt, M. J.; Palazzolo, A. M. E.; Lehmann, J. W.; Morehouse, G. F.; Burke, M. D. *Science* **2015**, *347*, 1221.

(138) Hammershøj, P.; Kumar, E. K. P.; Harris, P.; Andresen, T. L.; Clausen, M. H. *Eur. J. Org. Chem.* **2015**, *2015*, 7301.

(139) Chen, S.; Slattum, P.; Wang, C.; Zang, L. *Chem. Rev.* **2015**, *115*, 11967–11998.

(140) Tang, X.; Liu, W.; Wu, J.; Lee, C.-S.; You, J.; Wang, P. *J. Org. Chem.* **2010**, *75*, 7273.

(141) Wu, C.; Xiao, Z.; Wang, L.; Li, G.; Zhang, X.; Wang, L. *Catal. Sci. Technol.* **2021**, *11*, 1965.

(142) Wu, R.; Wiegand, K. R.; Wang, L. *J. Chem. Phys.* **2021**, *154*, 054705.